BIOINSPIRED COATINGS BASED ON LIPID NANOCARRIERS FOR TARGETED DRUG DELIVERY

Angela Gabriela PĂUN[1], Cristina DUMITRIU[1], Nicoleta BADEA[1], Cristian PIRVU*[1]

The biocompatibility of implant biomaterials is affected by surface bio-interfacial interactions with biomacromolecules, such as cell adhesion, protein adsorption, and biofilm formation. Our goal was to enhance the bioactivity of pure titanium samples by coating them with a biocompatible polydopamine film derived from mussel-inspired. We also used nanostructured lipid carriers (NLC), a second generation of lipid nanoparticles, as a delivery system for Indomethacin (Ind). To reduce swelling and discomfort caused by tissue lesions, Ind is an effective non-steroidal anti-inflammatory drug with antipyretic properties. The aim of applying this polydopamine film to titanium surfaces was to improve the binding efficiency of Ind and NLC-Ind. The key advantage of using nanocarriers is their ability to release the drug gradually. NLC-Ind were produced by high shear homogenization (HSH) coupled with high-pressure homogenization technique (HPH). The deposition of NLC and NLC-Ind onto implantable titanium surfaces is a novel approach that this study presents and discusses, offering a new perspective to the field. These samples also outperform the unmodified titanium in terms of corrosion resistance. Embedded in lipid nanocarriers, indomethacin exhibits prolonged release.

Keywords: Polydopamine, Indomethacin, Nanostructured lipid carriers, anti-inflammatory release.

1. Introduction

Implant biomaterials' biocompatibility is influenced by bio-interfacial interactions between the surface and biomacromolecules such as cell adhesion, protein adsorption, and biofilm formation. Titanium and its alloys have excellent physiological and mechanical properties (mechanical strength, high corrosion resistance, and low elastic modulus) [1, 2]. Thus, they have been widely investigated for a variety of biomedical applications such as bone plates, osteosynthesis plates, dental implants, subperiosteal implants, craniofacial implants and hip prosthesis [3]. Nevertheless, the inherent biological inertness and the absence of antimicrobial activities in titanium and its alloys present challenges for researchers [4, 5]. Thus, many methods of modifying titanium surfaces are utilized to increase their biological performance [6]. The advanced technology of surface

[1] Faculty of Chemical Engineering and Biotechnologies, National University of POLITEHNICA Bucharest, Romania, corresponding author's e-mail: cristian.pirvu@upb.ro

modification for bone biosubstitutes offers the potential to imbue them with multiple functionalities, aligning with the requirements of bone regeneration, including cell affinity, material biocompatibility, nontoxicity, and biodegradability [7]. Physical modification involves the deposition of bioactive materials (hydroxyapatite and chitosan) using various methods. Chemical functionalization includes the use of polydopamine (PD), thiols, and silanes, while biological modifications involve the application of biomacromolecules such as peptides and proteins [1].

However , surface modification inspired by polymerized dopamine (PD), an adhesive protein, has emerged as a straightforward, safe, efficient, and cost-effective alternative for addressing the needs of bone tissue engineering [7]. Notably, PD is characterized by its excellent biocompatibility, hydrophilicity, non-toxic and biodegradable nature, and it possesses the ability to modify its adhesive properties in the presence of amino acids [8, 9]. Consequently, PD can serve as a coating material to enhance the adhesive strength and biocompatibility of biomaterial surfaces [8, 10]. Many studies have indicated that applying polydopamine coatings on biomaterials leads to enhanced biocompatibility, increased resistance to cytotoxicity, and improved antibacterial activity [10-12]. However, the application of PD as an anti-inflammatory agent to treat acute inflammation-induced injury has not yet been demonstrated [13].

Indomethacin was approval from the US Food and Drug Administration in 1965 [14]. Ind (also known as 1-(chlorobenzoyl)-5-methoxy-2-methylindole-3-acetic) is a potent non-selective, non-steroidal anti-inflammatory agent. It exhibits significant strength and has a comparable effect to phenylbutazone. Additionally, it possesses antipyretic action, reducing pain or inflammation in tissue lesions [15, 16]. Indomethacin is soluble in acetone (40mg/ml), ethanol (20mg/ml), ether, and chloroform (50mg/ml). It remains stable in neutral and slightly acidic environments but is insoluble in water [17] .

The design of drug delivery systems enhances drug efficacy by improving stability and bioavailability. Transporter systems with nanometric dimensions can protect and enhance the intrinsic characteristics of the encapsulated active substance, allowing for targeted delivery. In drug delivery, nanoencapsulation technology represents a smart approach to achieving effective biodistribution. This capability stems from precise control over release, preventing drug degradation, enhancing the penetration efficiency of the active molecule, and averting toxic effects. The nature of the carrier systems plays a crucial role in selecting the appropriate drug encapsulation method. Novel nano-sized transporter systems have been developed for the transport of anti-inflammatory drugs [17].

Nanostructured lipid carriers (NLC), the second generation of lipid nanoparticles, are delivery systems for sensitive synthetic and natural drugs with applications in pharmaceutics [18-20], cosmetics [20, 21] and food [22] domains.

These lipid nanoparticles systems possess a bioavailability enhancement by increasing the permeability and mucoadhesive property of drug and permits extended release at the target and minimize dose dependent side effects [23, 24].

In this study, we applied a biocompatible polydopamine coating derived from mussel-inspired sources on pure titanium samples, aiming to increase their bioactivity. In the same time, the binding efficiency of indomethacin (Ind) and NLC-Ind onto titanium surfaces was improved by the presence of dopamine film deposited on titanium substrate. The employment of nanocarriers is based on their capacity to gradually release the drug over an extended period. The novelty of this research consists in the deposition NLC and NLC-Ind onto implantable titanium surfaces, a methodology that is introduced and discussed for the first time in specialized literature, contributing to a new perspective to the field.

2. Experimental section

2.1 Materials

Titanium (Ti), with a purity of 99.7 % and a thickness of 0.1 cm (1 cm x 1cm) used as a support material, was supplied by the company Alpha Aesar.

Sigma Aldrich provided trizma® base, dopamine hydrochloride (98% purity), hydrochloric acid, Indomethacin (Ind), Ethylene glycol anhydrous (99,8% purity), Dimethyl sulfoxide, Disodium phosphate, Dihydrophosphate sodic, ethyl 1,4-phthalazinedione (Luminol, 97% purity), Tris[hydroxymethyl] aminomethane (99.8% purity), Poloxamer 188/poly(ethylene glycol)-block-poly(propylene glycol)-block-poly(ethylene glycol) (99 % purity), L-α-phosphatidylcholine.

Hydrogen peroxide 30 % (98 % purity), polyoxyethylene sorbitan monolaurate (Tween 20) (97% purity) were purchased from Merck, glycerol monostearate (GM) was obtained from Cognis GmbH (99 % purity), and cetyl palmitate (CP) was purchased from Acros Organics. The raspberry oil (Rbo) was obtained from the Elemental Company. Chimreactiv supplied us with ethyl alcohol and acetone. A Millipore Direct-Q UV3 water purification system was used to produce purified water. All the chemicals were analytical grade reagents that didn't require any additional purification.

2.2 Modification of the titanium surface

2.2.1. Lipid nanocarriers synthesis (NLC)

The lipid nanocarriers with and without indomethacin were produced by high shear homogenization (HSH) coupled with high-pressure homogenization technique (HPH) according to a method described by authors Lacatusu et al. [18, 19]. The lipid phase consisting of cetyl palmitate, glycerol monostearate and raspberry oil (35:35:10 % w) melted at a temperature of 75^{o}C, was added over the aqueous phase containing 2.5 % surfactant (lecithin, poloxamer and Tween 20) at

the same temperature, and was magnetic stirred for 15 minutes. The pre-emulsions were homogenization to HSH at 12000 rpm, for 1 min, and HPH for 6 homogenization cycles at 500 bars. The dispersions of NLCs were lyophilized using a Christ Alpha 1-2 LD Freeze Dryer (-55 ^{o}C, 0,04 mbar, 72 h). The composition of each NLC formulation is given in Table 1.

Table 1

Compositional aspects of NLCs loaded with Indomethacin

Type and composition. NLC*	Solid lipids **, %		Raspberry seed oil (Rso)	Indomethacin (Ind)
	GM	CP		
NLC	3.5	3.5	3	-
NLC-Ind	3.5	3.5	3	0.5

*2.5% surfactant mixture Tween 20: Phosphatidylcholine: Poloxamer.
**The values are expressed in w / w (% composed of the total weight of the aqueous dispersion);

2.2.2. Polydopamine synthesis

The polydopamine solution was prepared by mixing 0.945 g dopamine and 100 ml TRIS buffer. The TRIS buffer with pH=8.5, contains trizma® base 0.2 M, HCl 0.2 M and distilled water.

2.2.3. Deposition of polydopamine and lipid nanocarriers on the titanium surface

Firstly, titanium plates were subjected to ultrasound treatment in an Elma-TI-H-5 ultrasonic bath for 15 minutes each for cleaning in ultrapure water and degreasing in ethanol and acetone. They were allowed to dry in the air [25, 26].

In a sterile container, Ti samples were immersed at room temperature, in dark conditions, for 24 h in 10 mL in the polydopamine solution, previously obtained. Samples were wash with distilled water. The obtained sample was named **Ti/PD**.

In two sterile containers were obtained different solutions, one containing the NLC (0.01 g /10 mL ethanol) and the other NLC-Ind (0.01 g/10 mL ethanol). These solutions were ultrasonically treated for five minutes in order to improve the solubility of NLCs in ethanol. In parallel, a solution of indomethacin with the same concentration was made. Subsequently, Ti/PD samples were added in each sterile container. The process took place during 7 days in the dark, until complete evaporation of ethanol. Meanwhile, NLCs and indomethacin were deposited on the titanium surface through polydopamine bio-adhesive. The names for the modified substrates are **Ti/PD/NLC, Ti/PD/NLC-Ind and Ti/PD/Ind**.

In Fig. 1 is presented the working scheme used to modify the titanium surfaces.

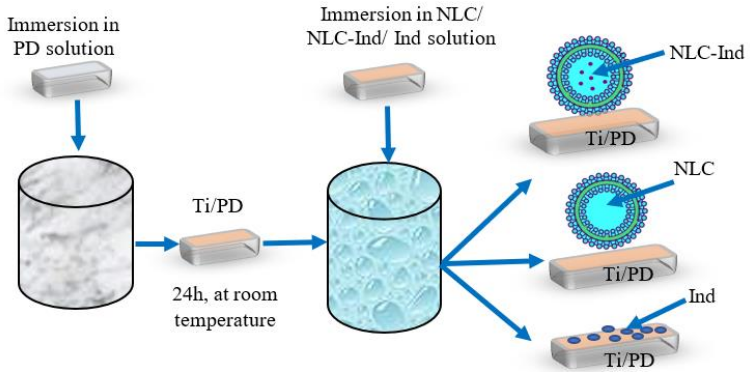

Fig. 1. The working scheme used to modify the titanium surfaces

2.3 ***Samples characterization***

The average diameters (Zave) and polydispersity index (PdI) of the NLCs were analysed by dynamic light scattering (DLS) using Zetasizer Nano ZS (Malvern Instruments Ltd., UK) at a scattering angle of 90° and at a temperature of 25°C.

The zeta potential (ξ) of NLC was determined with the same apparatus, using the electrophoretic light scattering technique. The NLC dispersions were diluted with purified water and the conductivity was adjusted to 50 µS/cm by adding a solution of 0.9 % NaCl. All measurements were performed in triplicate.

The entrapment efficiency for indomethacin (EE) in NLC was determinate used 0.05 g NLC-Ind lyophilized dispersed into 2 mL water and the suspension was centrifuged for 15 min at 13000 rpm (Sigma 2K15, Germany). The supernatant containing the unloaded indomethacin was analyzed by High-performance liquid chromatography (HPLC), using an HPLC-Jasco 2000 liquid chromatograph provided with UV detector, λ= 213 nm, Nucleosil C18 column (5 µm, 25 x 0.4 mm). The eluent used was ACN: H_3PO4, 0.5 % (50:50), flow rate of 1 mL/min, retention time for indomethacin 6.74 min. The concentrations of indomethacin were calculated using the calibration curve in the concentration range of 0.01–0.1 g/L and the correlation coefficient (R^2) is 0.9998.

The entrapment efficiency of indomethacin (EE) was calculated using the equation:

$$EE\% = \frac{Initial\ amount\ of (Indo)\ into\ NLCs - Amount\ of\ free\ (Indo)}{Initial\ amount\ of\ (Indo)\ into\ NLCs} \cdot 100 \quad (1)$$

The antioxidant activity (AA) was determined using un chemiluminometer Turner Desing and a chemiluminescence systems consisting by luminol (10^{-5} M), H_2O_2 (10^{-5} M) at pH =8,6 (Tris-HCl).

Information about surface morphology was obtained with a Scanning Electron Microscopy (SEM). Using a Quanta Inspect F or Nova NanoSEM 630 (FEI Company, USA), top views were obtained.

FTIR Spectrum 100 (PerkinElmer USA) spectrometer was used to acquire the infrared spectra. The range of 1400-4200 cm^{-1} was used for all measurements, which were averaged from four scans with a 4 cm^{-1} resolution.

The electrochemical characterization of the samples was performed in an electrochemical cell with a three-electrode system (Ti or Ti coated electrode - working electrode, Ag/AgCl 3M KCl electrode - reference electrode (Metrohm) and 3 mm Pt rod electrode - counter electrode) (Metrohm)]. Electrochemical measurements were performed with a potentiostat/galvanostat model PGSTAT 302N (Metrohm, Autolab, The Nederlands), using the Nova 1.11 software. Tafel tests were performed with a scan rate of 2 mV/s, being recorded between -260 mV and +150 mV domain compared to the open-circuit potential (OCP). The measurements were registered in NaCl solution 0.9 %, under ambient conditions. All measurements were enregistered at room temperature using an amplitude of 10 mV relative to the AC potential and a frequency range of 0.1 - 10^5 Hz for the electrochemical impedance spectra (EIS). The cyclic voltammetry curves were recorded, with a scan rate of 100 mV/s and a potential between - 1.5 V and 1 V.

The surface wettability was examined with a CAM 100 Optical Contact Angle Meter device (KSV Instruments), using the Sessile Drop method. There were used three different solvents (water, EG and DMSO). A photo-taking device and an image-processing program were used to capture the drop-image. The shape of the drop was used to calculate the contact angle (θ). A small amount of liquid, approximately 3–5 μL, was created with a Hamilton syringe and placed on the surface. The average value was computed after recording 4 contact angles values for each measurement, on different spots on the sample surface. The study was conducted at a temperature of 25 °C.

*2.4 **Indomethacin release studies***

For release studies, Ti/PD samples were immersed in 10 mL ethanolic solution of NLC-Ind and Ind, having the same concentration and allowed to evaporate. After evaporation, the samples were placed in 5 mL receptor medium ethanol: phosphate buffer (50:50), pH 7.4. At time intervals, a volume of 0.5 mL was collected from this solution and 0.5 mL receptor medium solution was introduced. The concentration of indomethacin released from the two samples was monitored by HPLC according to the method described in point 2.3. The mechanism of indomethacin release was stablished by fitting the release data using five mathematic model: first order: $\ln(100 - \%R) = k_1 t$; Higuchi: $\%R = k_2 \sqrt[2]{t}$; Hixson–Crowell: $\sqrt[3]{100 - \%R} = k_3 t$, Korsmeyer-Peppas: $\%R = k_4 \sqrt[n]{t}$ where, %R is percent of Indo release at time t; $k_1 \div k_4$ are the rate constants for first order, Higuchi

and Hixson-Crowell respectively; n is the release exponent. The mathematical models' equations with the biggest R^2 were selected as the best release kinetic model.

3. Results and discussion

3.1 Characterization of NLC

The size characterization of NLC was determined using dynamic light scattering technique. The NLC samples presented a relatively narrow distribution of the lipid particles, the size between 117 and 137 nm the polydispersity indices being between 0.17 and 0.19. The average diameters of simple NLC were 137.0 ± 0.8 nm and 0.188 (PdI) *versus* 118,1 ± 0.86 nm and 0.193 (PdI) for NLC-Ind.

These NLC samples present a good physical stability, and zeta potential values were -46.7 mV for NLC free and -49 mV for NLC-Ind. The values of the electrokinetic potential demonstrate the existence of repulsion phenomena between lipid particles in aqueous suspension, favorable for preventing the aggregation of simple lipid nano-carriers ~~free~~ or loaded with anti-inflammatory drug. Table 2 presents comparatively the size and electrokinetic potential of NLC samples.

Table 2

The size and zeta potential of NLC samples

Samples	Z_{ave} [nm]	PdI	ξ [mV]	EE	AA
NLC	137.0 ± 0.80	0.188 ± 0.007	-46.7 ± 0.874	-	87.61 ± 0.75
NLC-Ind	118.1 ± 0.86	0.193 ± 0.016	-49.0 ± 1.643	70.79 ± 1.42	92.88 ± 0.14

The entrapment efficiency of indomethacin in NLC was 70.8 ±1.42%, and this value indicates a more difficult accommodation of indomethacin in the imperfections of the lipid core [27-30]. The NLC samples present a good capacity for scavenger oxygen radicals and the antioxidant activity is due to the phytochemicals present in the raspberry oil used in the synthesis of NLC [31].

3.2 Structure and morphology of Ti substrate with modified surfaces

Fig. 2 present SEM image for all samples with modified surfaces. Fig. 2a-b shows the deposition of polydopamine as a homogenous coating on the titanium surfaces. The film appears thin, and scratches from the polishing step are noticeable. Fig. 2c-d shows the SEM images for the Ti/PD/Ind sample. The SEM images reveal the presence of uniformly distributed Indomethacin crystals on the titanium surface. Additionally, it is evident that these crystals are very well anchored to the titanium surface. This strong adhesion is attributed to the presence of polydopamine, which

is identifiable in the SEM images as a thin film. In Fig. 2d, it is observed that the indomethacin crystals exhibit a tubular shape and are uniformly distributed. These crystals vary in sizes and diameters.

Figs. 2e-f show the deposition of Nanostructured Lipid Carriers (NLCs) as agglomerates on the titanium surface with flower-shaped appearance. Similarly, NLCs containing indomethacin may be observed in Fig. 2 g-h. It seems that the particles are arranged in clusters with a spherical form. They were made of many layers and seems to be porous. The drug loading is improved, and more spaces are provided for the drug to be embedded in the porous structure of NLCs. This characteristic may promote the release of drugs from nanoconfinements. Consequently, it is confirmed that both NLC and NLC-Ind were deposited on the titanium surface in the form of agglomerates, with polydopamine serving as the binding agent.

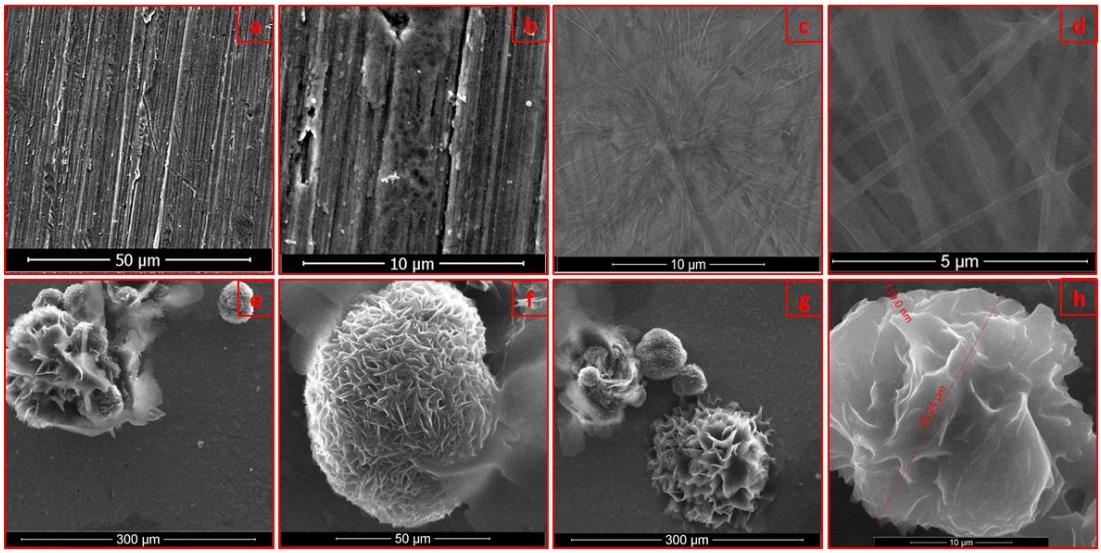

Fig. 2. SEM images corresponding to the sample: a, b) Ti/PD; c, d) Ti/PD/Ind; e, f) Ti/PD/NLC; g, h) Ti/PD/NLC-Ind

*3.3 **Fourier transform infrared***

In Fig. 3a, in the specific spectrum of the Ti/PD sample, the peaks are assigned as follows: the -OH vibration is at 3324 and 3467 cm^{-1}, and the signal 1524 cm^{-1} is attributed to the various vibrations -NH [32]. Normally, the NLC has the specific peaks at 2916, 2848, 1734 and 1181 cm^{-1} [33]. In Fig. 3b, in the specific spectrum to the NLC sample it can be observed that the peaks to this sample are found at 2915, 2849, 1733 and 1469 cm^{-1}. Also, it can be observed that Fig. 3c is identical to Fig. 3b. This shows that the lipid nanocarriers are very well adhered to

the titanium surface. In Fig. 3c don't present polydopamine-specific peaks, indicating that the NLCs are uniformly deposited.

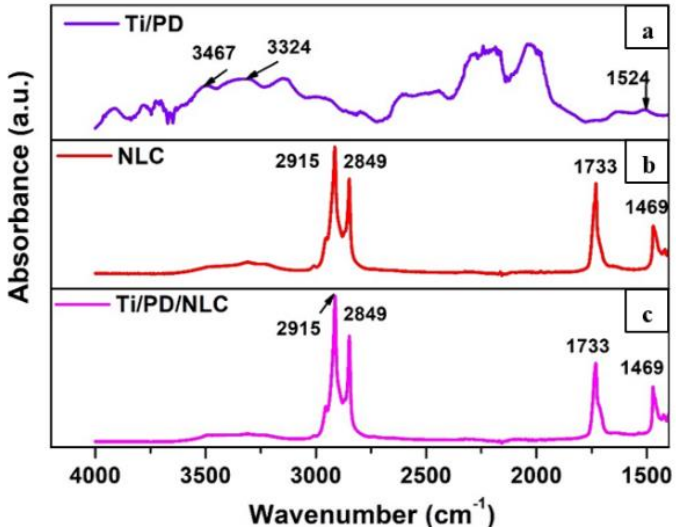

Fig. 3. FT-IR images of the samples: a. Ti/PD; b. NLC; c. Ti/PD/Ind

Fig. 4 shows the specific spectra for Ti/PD, Ind, NLC-Ind and Ti/PD/NLC-Ind samples. In Fig. 4a, the specific peaks of the Ti-PD sample are found at 3324, 3467 and 1524 cm^{-1}. In Fig. 4b, the specific peaks of indomethacin are visible: at 1716 cm^{-1} is the C = O groups, the 1686 cm^{-1} is also specific for the C = O group linked to the aromatic nuclei. The peak from 1590 cm^{-1} is specific to benzene C=C groups [34]. In NLC-Ind and Ti/PD/NLC-Ind samples, indomethacin specific spectra are not visible (Fig. 4c and 4d). This may be due to the very low concentration of indomethacin.

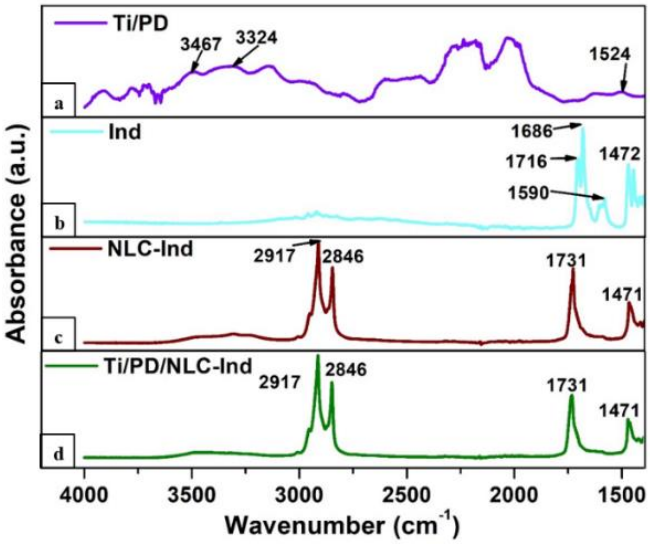

Fig. 4. FT-IR images of the samples: a. Ti/PD; b. Ind; c. NLC-Ind; d. Ti/PD/NLC-Ind

The Ti/PD/Ind sample (Fig. 5c) presents similar peaks at 1716 cm^{-1} (attributed to C = O), 1686 cm^{-1} (attributed to C = O in aromatic nuclei), and 1590 cm^{-1} (associated with benzene C=C groups) [34]. The spectrum of indomethacin powder, Fig. 5b, exhibits peaks at the same wavenumbers, indicating the presence of indomethacin on the titanium surface.

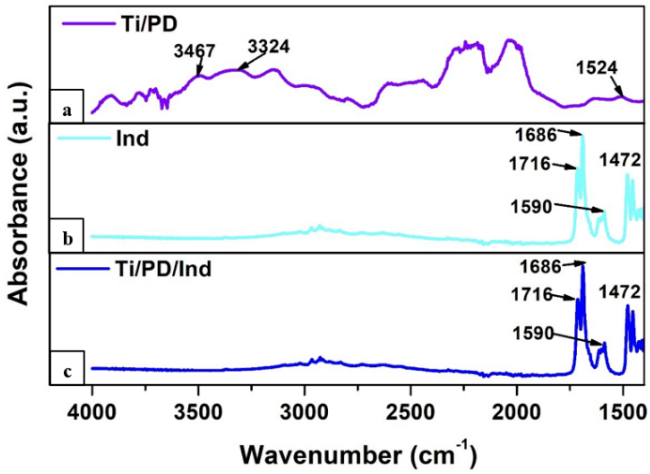

Fig. 5. FT-IR images of the samples: a. Ti/PD; b. Ind; c. Ti/PD/Ind

3.4 ***Surface wettability***

Wettability is an important property of the biomaterial. Combined with other surface features, such as energy, topography and surface chemistry, wettability influences the processes from the biomaterial-tissue interface [35, 36].

Surface energy has a crucial role in many biological processes, considering the interaction of cells or bacteria with the biomaterial surface after implantation. Measuring the contact angle with different solvents allows the determination of the hydrophilic or hydrophobic character of the surface. Literature studies show that hydrophilic surfaces favor better implant-cell interaction, rejecting bacteria [37].

Table 3

Contact angle values in different solutions

Samples	Contact Angle [°]			Surface energy [mJ /m^2]
	Water	Ethylene glycol	DMSO	
Ti	80.8 ± 4.5	54.7 ± 3	36 ± 2	37.956
Ti/PD	55.6 ± 4	35 ± 5	15.6 ± 2	45.018
Ti/PD/Ind	22.8 ± 2	18.4 ± 1	5.3 ± 1	67.077
Ti/PD/NLC	56.2 ± 0.4	49.8 ± 1	34.8 ± 1	42.54
Ti/PD/NLC-Ind	40.4 ± 1.2	32.6 ± 1.3	21 ± 0.2	55.188

For the samples obtained in this study, the contact angle values for the dispersive component (water, ethylene glycol and DMSO) are shown in Table 3. It can be observed that by coating the titanium surface, the contact angle decreases. Also, all samples have contact angle values less than 90 °, indicating that they have a hydrophilic character. The Ti/PD/Ind sample has the most hydrophilic surface. Regarding the surface energy, it can be observed that its increase occurs when the titanium surface is modified. According to literature studies, surfaces with energy higher than 30 mJ/m^2 improve cell-biomaterial interaction [38]. In this study, all samples have surface energy superior to the suggested minimum value for biomedical applications. The surface energy of the materials varied between 37 and 67 mJ/m^2, which could influence the activity of ALP (alkaline phosphatase).

3.5 ***In vitro indomethacin release***

Fig. 6 shows the percentage variation of anti-inflammatory drug released (% R) over time for the two systems. There are differences between the two analyzed samples, in the case of the Ti/PD/NLC-Ind sample, a gradual release of the drug into the environment (phosphate buffer and ethanol) is ensured, due to the encapsulation of indomethacin in the lipid nanocarriers system, compared to the Ti/PD/Ind sample. In the case of the sample on which only the drug was deposited, the quantity of indomethacin released is 1.35 times higher than for the Ti/PD/NLC-Ind system.

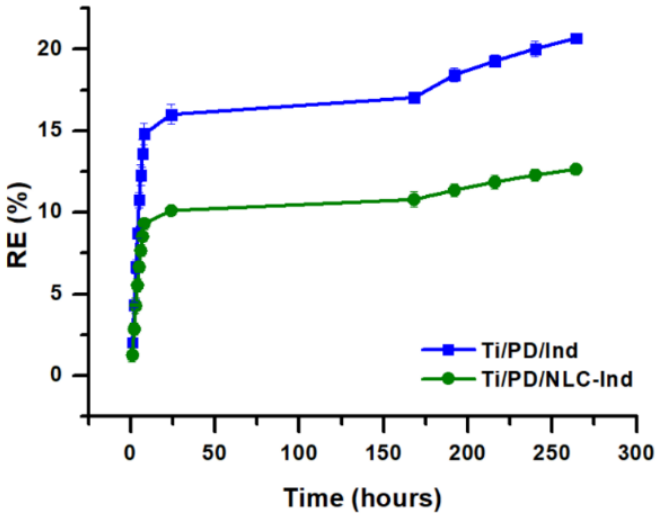

Fig. 6. The quantity of indomethacin released in over time

In order to determine the release kinetics, depending on the encapsulation mode of indomethacin, the cumulative quantity of drug released in the 1 – 8 h range (excluding the plateau between 8h and 24 h) was fitted with different kinetic models. The correlation coefficient (R^2) and the release rate constant (k) of indomethacin are shown in Table 4. *In vitro* release kinetics study of indomethacin in the two systems performed on different models showed that the drug delivery corresponds to the Higuchi model.

Table 4

Correlation coefficient (R^2) and release rate constant (k) of indomethacin

Samples	Zero order		First order		Higuchi		Hixson-Crowell		Peppas-Korsmeyer		
	R^2	k_0	R^2	k_1	R^2	k_2	R^2	k_3	R^2	k_4	n
Ti/PD/Ind	0.985	1.843	0.989	0.020	0.997	7.229	0.988	0.029	0.992	0.774	1.037
Ti/PD/NLC-Ind	0.986	1.142	0.988	0.012	0.999	4.483	0.987	0.017	0.990	0.328	1.048

The kinetics found in the Ti/PD/NLC-Ind release system ensure a continuous release rate of the drug, in a reduced concentration (through diffusion-controlled processes). Therefore, the encapsulation of indomethacin in lipid nanocarriers systems is advantageous due to the decrease in drug dose, which ensures a reduction of side effects as well as a prolonged therapeutic effect.

*3.6 **Electrochemical characterization***

3.6.1 Tafel analysis

The Tafel diagram is shown in Fig. 7. It can be observed that by modifying the titanium surface, the electrode potentials were displaced to more electropositive values and corrosion currents toward lower values than the untreated titanium.

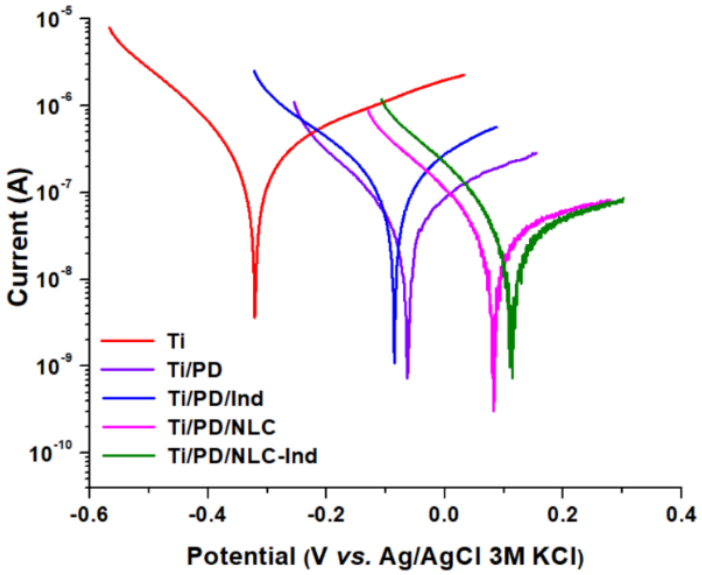

Fig. 7. Tafel diagrams recorded in NaCl 0.9%

Using the NOVA software, by extrapolating the cathodic and anodic curves, the main corrosion parameters were determined (Table 5). Moreover, the protection's efficacy was determined using the formula described in our study [39].

Table 5

The main corrosion parameters using NOVA software

Samples	Corrosion potential (V)	Corrosion current density (A/cm^2)	Corrosion rate (mm/year)	Protection efficiency (%)
Ti	-0.32	$8.74 \cdot 10^{-7}$	$7.60 \cdot 10^{-3}$	-
Ti/PD	-0.06	$4.37 \cdot 10^{-7}$	$3.80 \cdot 10^{-3}$	50
Ti/PD/Ind	-0.08	$5.40 \cdot 10^{-7}$	$4.70 \cdot 10^{-3}$	38
Ti/PD/NLC	0.08	$1.21 \cdot 10^{-7}$	$1.05 \cdot 10^{-3}$	86
Ti/PD/NLC-Ind	0.11	$3.92 \cdot 10^{-7}$	$3.41 \cdot 10^{-3}$	55

Corrosion potential is a crucial metric for assessing corrosion. It is observed that all the modified samples have a more electropositive corrosion potential than the untreated titanium which indicates that their surface is more stable to corrosion. NLC and NLC-Ind samples are the most stable corrosion samples.

Corrosion resistance is inversely related to corrosion rate, hence higher values of corrosion current density indicate weaker corrosion resistance Ti/PD/NLC and Ti/PD/NLC-Ind have the lowest corrosion current density.

Only the simple coating of the polydopamine film decreases the value of the corrosion rate. Polydopamine shields pure titanium against corrosion by creating a barrier as a thin film that stops the transfer of oxygen ions and titanium ions. The embedding of Indomethacin in the polydopamine film doesn't significantly change the value of the corrosion rate ($4.7 \cdot 10^{-3}$ mm/year, compared to $3.8 \cdot 10^{-3}$ mm/year). The lowest value was recorded for samples with lipid nanocarriers, with and without Indomethacin, demonstrating their improved thermodynamic stability.

3.6.2 Impedance diagrams

The normalized Nyquist diagrams corresponding to the coated samples and Ti substrate are shown in Fig. 8. A reduced diameter of the semicircle in a Nyquist plot indicates a material with lower corrosion resistance. The smallest semicircle is seen while examining Ti sample. All samples with modified surfaces are more stable than Titanium.

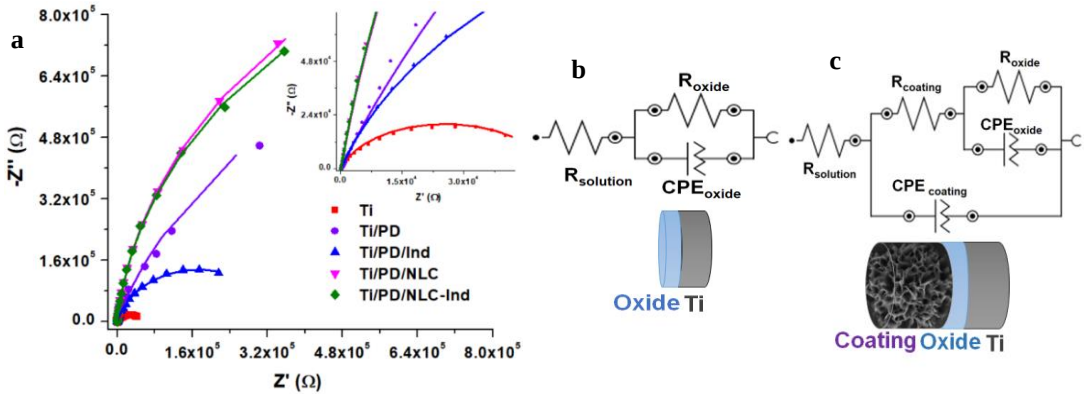

Fig. 8. a) Impedance diagrams of the modified Ti samples b) Equivalent circuits used to fit the EIS data for Ti and c) Circuits used to fit EIS data for coated samples

Two equivalent circuits (Fig. 8 b-c) were proposed for fitting data. For titanium, was used the bioliquid resistance - NaCl 0.9 % ($R_{solution}$), in series with a circuit corresponding to the oxide layer consisting of a constant phase element (CPE_{oxide}) in parallel with an oxide resistance (R_{oxide}).

For the samples with modified surface, it was necessary to add a characteristic circuit to the coating layer, consisting of a resistance ($R_{coating}$) in parallel with a constant phase element ($CPE_{coating}$). The data obtained with the Nova software can be found in Table 6.

Table 6

Parameters obtained from data fitting

Parameters Samples	$R_{solution}$ (Ω)	$R_{coating}$ (Ω)	$CPE_{coating}$		R_{oxide} (Ω)	CPE_{oxide}		X^2
			Y_0 ($S*s^n$)	N		Y_0 ($S*s^n$)	N	
Ti	125	-	-	-	$2.00\cdot10^{+6}$	$2.05\cdot10^{-6}$	0.90	0.23
Ti/PD	143	$401\cdot10^{+3}$	$2.22\cdot10^{-5}$	0.79	$2.50\cdot10^{+6}$	$9.0\cdot10^{-6}$	0.99	0.32
Ti/PD/Ind	107	$381\cdot10^{+3}$	$2.26\cdot10^{-5}$	0.82	$2.33\cdot10^{+6}$	$1.1\cdot10^{-6}$	0.86	0.3
Ti/PD/NLC	132	$570\cdot10^{+3}$	$1.53\cdot10^{-5}$	0.93	$2.13\cdot10^{+6}$	$8.9\cdot10^{-6}$	0.86	0.4
Ti/PD/NLC-Ind	136	$441\cdot10^{+3}$	$1.57\cdot10^{-5}$	0.92	$2.09\cdot10^{+6}$	$9.0\cdot10^{-6}$	0.85	0.6

It was observed that the resistance values were about the same for the solution (0.9 % NaCl), around 100 Ω. From Table 6 it is observed that by depositing dopamine (Ti/PD) and incorporating NLCs, the resistance of the barrier oxide layer increases compared to the titanium substrate. By simply incorporating indomethacin into dopamine (Ti/PD/Ind), the resistance decreases slightly compared to that of the Ti/PD sample but is higher than that of untreated titanium.

An additional barrier against corrosion is generated by increasing the $R_{coating}$, which hinders the discharge of solute ions. Ti/PD/NLC sample exhibited the highest resistance of the coating layer, showing superior resistance to corrosion, as seen by its larger semi-circle diameter compared to the other specimens. These observations align with the findings of Tafel polarization results. Indomethacin decreases this resistance, even if it is incorporated into the dopamine film or lipid nanocarriers.

The variables Y (0) and N, which denote the admittance of an ideal capacitance and an empirical constant, respectively, characterize CPE. N is an empirical constant with a range of values from 0 to 1. Where N denotes the exponential component, the CPE equation indicates the deviation from the pure capacitance as a theory. When N is set to zero, the CPE demonstrates properties similar to those of a pure resistor, where Y_0 equals R. When N is equal to 1, however, the CPE exhibits characteristics of a pure capacitor. For both layers, the barrier oxide and the coating, the values of N are above 0.7, indicating a pseudocapacitive behavior of the layers.

3.6.3 Cyclic voltammetry

The cyclic voltammetry curves are shown in Fig. 9. From these curves, good corrosion resistance is observed for all studied electrodes. Anodic currents are higher for untreated titanium. The nature of the polarization curves indicates a stable passive behavior (without any active - passive transition) for all samples with modified surface. On the cathodic curves, the current has lower values than the one on the anodic curve. The cathodic currents for the samples with indomethacin are

higher, due to its antioxidant activity. This may explain the lower values of the impedance oxide layer resistances. Thus, the indomethacin slightly reduces the resistance of the oxide layer.

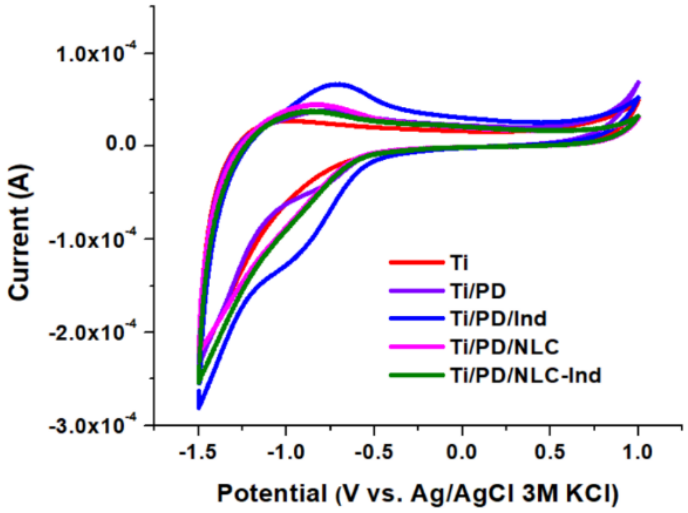

Fig. 9. Cyclic voltammetry diagrams

Table 7 demonstrates that the C_{dl} surface capacitance of Ti/PD was 211.34 µF/cm^2, significantly greater than that of Ti (163.66 µF/cm^2). It is evident that when Ti/PD surfaces change using NLC, the C_{dl} value decreases (181.46 µF/cm^2). This may be associated to the decrease in surface energy, which can be determined by reducing the active surface area.

Table 7

C_{dl} values calculated from CV plots for Ti and coated samples

Sample	C_{dl} (µF/cm^2)
Ti	163.66
Ti/PD	211.34
Ti/PD/Ind	272.77
Ti/PD/NLC	181.46
Ti/PD/NL-Ind	185.84

The titanium surface modification with indomethacin increases the C_{dl} value and improves the surface's hydrophilicity, improving charge transfer at the interface and the formation of electrical double layers. As a result, ion diffusion has a substantial influence on the electrochemical capacity of the deposited structures, and charge transfer may be increased. This could imply that the ion absorption/desorption mechanism at the electrolyte / nanostructured surface interface is more efficient.

Electrochemical analyses demonstrated that the modified titanium samples were more stable.

4. Conclusions

In order to improve the interaction of the implant-biological environment, the titanium surface has been modified. These surfaces were obtained by depositing Indomethacin and lipid nanocarriers containing indomethacin, for local releases of the drug.

All samples with modified surfaces are expected to be biocompatible due to their hydrophilic character (contact angle is less than 90 °) and from the surface energy point of view. If the surface energy exceeds 30 mJ /m^2, the scientific world considers that the surface fulfills one of the biomedical standards.

Analyzing the obtained results with this method it was shown that, regardless of the surface modification made on the titanium, the surface energy increased. These samples also outperform the unaltered titanium in terms of corrosion resistance. When lipid nanocarriers encapsulate indomethacin, its release was prolonged.

Finally, for local drug administration, the Ti/PD/NLC-Ind system proved to be the optimal solution.

As a perspective, investigations will be conducted to assess the stability and sustained drug release over an extended period. *In vivo* tests on human cells are also planned to observe the interactions produced and get thorough insights into the biocompatibility of the newly designed surfaces.

Other drugs will be released from various nanocarriers in Fusayama simulant saliva (pH 5.5), as in stressful body conditions the physiological pH moves towards acidity.

Acknowledgement

The SEM analyses was funded by European Regional Development Fund through Competitiveness Operational Program 2014–2020, Priority axis 1, Project No. P_36_611, MySMIS code 107066

R E F E R E N C ES

[1]. *L.M. Pandey*. Design of biocompatible and self-antibacterial titanium surfaces for biomedical applications. Curr Opin Biomed. 2023;25:100423.

[2]. *G. Senopati, et al.* Recent Development of Low-Cost β-Ti Alloys for Biomedical Applications: A Review. Metals. 2023;13(2):194.

[3]. *P. Pesode, et al.* A review—metastable β titanium alloy for biomedical applications. J Eng Appl Sci. 2023;70(1):25.

[4]. *P. Pesode, et al.* Titanium alloy selection for biomedical application using weighted sum model methodology. Mater Today: Proc. 2023;72:724-8.

[5]. *M.H. Qi, et al.* Novel bioactive Ti-Zn alloys with high strength and low modulus for biomedical applications. J Alloys Compd. 2023;931:167555.

[6]. *P. Jiang, et al.* Advanced surface engineering of titanium materials for biomedical applications: From static modification to dynamic responsive regulation. Bioact Mater. 2023;27:15-57.

[7]. *S. Huang, et al.* Polydopamine-Assisted Surface Modification for Bone Biosubstitutes. Biomed Res Int. 2016;2016:2389895.

[8]. *J.-J. Lee, et al.* Effects of polydopamine coating on the bioactivity of titanium for dental implants. IJPEM. 2014;15(8):1647-55.

[9]. *H. Xu, et al.* Smart polydopamine-based nanoplatforms for biomedical applications: state-of-art and further perspectives. Coord Chem Rev. 2023;488:215153.

[10]. *S.H. Choi, et al.* Enhanced antibacterial activity of titanium by surface modification with polydopamine and silver for dental implant application. J Appl Biomater Funct Mater. 2019;17(3):2280800019847067.

[11]. *Y. Xu, et al.* Bioinspired polydopamine hydrogels: Strategies and applications. Prog Polym Sci. 2023;146:101740.

[12]. *T. Ma, et al.* Applications of polydopamine in implant surface modification. Macromol Biosci. 2023;23(10):2300067.

[13]. *H. Zhao, et al.* Polydopamine nanoparticles for the treatment of acute inflammation-induced injury. Nanoscale. 2018;10(15):6981-91.

[14]. *A. Shete, et al.* Enhancement of solubility and dissolution rate of indomethacin by chitosan based solid dispersion technique. JCPR. 2015;5(2):1463.

[15]. *V. Sridhar*. Solubility improvement by solid dispersion and their characterization: indomethacin and phenytoin: University of Toledo; 2013.

[16]. *I. Krasnuk, et al.* Application of indomethacin in medicine and pharmacy. Вестник Российской академии медицинских наук. 2018;73(2):130-4.

[17]. *W. Badri, et al.* Elaboration of nanoparticles containing indomethacin: Argan oil for transdermal local and cosmetic application. J Nanomater. 2015;16(1):113-.

[18]. *S.P. Balguri, et al.* Topical ophthalmic lipid nanoparticle formulations (SLN, NLC) of indomethacin for delivery to the posterior segment ocular tissues. Eur J Pharm Biopharm 2016;109:224-35.

[19]. *I. Lacatusu, et al.* Multifaced role of dual herbal principles loaded-lipid nanocarriers in providing high therapeutic efficacity. Pharm. 2021;13(9):1511.

[20]. *L.V. Arsenie, et al.* Azelaic acid-willow bark extract-panthenol–Loaded lipid nanocarriers improve the hydration effect and antioxidant action of cosmetic formulations. Ind Crops Prod. 2020;154:112658.

[21]. *G. Niculae, et al.* Optimization of lipid nanoparticles composition for sunscreen encapsulation. UPB Sci Bull Ser B. 2013;75:79-92.

[22]. *M.H. Lee, et al.* Formulation and characterization of β-caryophellene-loaded lipid nanocarriers with different carrier lipids for food processing applications. LWT. 2021;149:111805.

[23]. *G. Badea, et al.* Naringenin improves the sunscreen performance of vegetable nanocarriers. New J Chem. 2017;41(2):480-92.

[24]. *Y.-Q. Zhao, et al.* Lipid-Based Nanocarrier Systems for Drug Delivery: Advances and Applications. Pharmaceutical Fronts. 2022;4(02):e43-e60.

[25]. *A.G. Păun*. TiO 2 Surfaces Modification for Amoxicillin Release Used in Dental Implantology. UPB Sci Bull Ser B. 2023;85:71-84.

[26]. *R. Irodia*. enhanced photocatalytic degradation of tetracycline by TiO_2 nanotubes coated with TiO_2 nanofibers. UPB Sci Bull Ser B. 2023;85(1):63-76.

[27]. *I. Lacatusu, et al.* Improved anti-obesity effect of herbal active and endogenous lipids co-loaded lipid nanocarriers: Preparation, in vitro and in vivo evaluation. Mater Sci Eng C 2019;99:12-24.

[28]. *I. Lacatusu, et al.* Marigold extract, azelaic acid and black caraway oil into lipid nanocarriers provides a strong anti-inflammatory effect in vivo. Ind Crops Prod. 2017;109:141-50.

[29]. *I. Lacatusu, et al.* Advanced bioactive lipid nanocarriers loaded with natural and synthetic anti-inflammatory actives. Chem Eng Sci. 2019;200:113-26.

[30]. *T. Hori, et al.* Crystal structure of anti-configuration of indomethacin and leukotriene B4 12-hydroxydehydrogenase/15-oxo-prostaglandin 13-reductase complex reveals the structural basis of broad spectrum indomethacin efficacy. J Biochem. 2006;140(3):457-66.

[31]. *G. Niculae, et al.* Rice bran and raspberry seed oil-based nanocarriers with self-antioxidative properties as safe photoprotective formulations. Photochem Photobiol Sci. 2014;13:703-16.

[32]. *R. Mrówczyński, et al.* Electron paramagnetic resonance imaging and spectroscopy of polydopamine radicals. J Phys Chem B. 2015;119(32):10341-7.

[33]. *A. Saupe, et al.* Structural investigations on nanoemulsions, solid lipid nanoparticles and nanostructured lipid carriers by cryo-field emission scanning electron microscopy and Raman spectroscopy. Int J Pharm. 2006;314(1):56-62.

[34]. *P. Tong, et al.* A study of amorphous molecular dispersions of indomethacin and its sodium salt. J Pharm Sci. 2001;90(12):1991-2004.

[35]. *F. Rupp, et al.* A review on the wettability of dental implant surfaces I: theoretical and experimental aspects. Acta Biomater. 2014;10(7):2894-906.

[36]. T. Ma, et al., editors. Effect of titanium surface modifications of dental implants on rapid osseointegration. Interface Oral Health Science 2016: Innovative Research on Biosis–Abiosis Intelligent Interface; 2017: Springer Singapore.

[37]. *T. Darmanin, et al.* Recent advances in the potential applications of bioinspired superhydrophobic materials. J Mater Chem A 2014;2(39):16319-59.

[38]. *A.G. Olaru, et al.* Biopolymers as intermediate layers for amoxicillin grafting on antibacterial surface. Surf Interfaces 2022;33:102224.

[39]. *A.G. Păun, et al.* Silk Fibroin/ZnO Coated TiO2 Nanotubes for Improved Antimicrobial Effect of Ti Dental Implants. Mater. 2023;16(17):5855.